

Electron diffraction from elliptical nanotubes

Zejian Liu ^a, Lu-Chang Qin ^{a,b,*}

^a Department of Physics and Astronomy, University of North Carolina at Chapel Hill, Chapel Hill, NC 27599-3255, USA

^b Curriculum in Applied and Materials Sciences, University of North Carolina at Chapel Hill, Chapel Hill, NC 27599-3255, USA

Received 21 November 2004; in final form 22 February 2005

Available online 17 March 2005

Abstract

A quantitative method for the structural determination by electron diffraction of nanotubes of elliptical cross-section is developed as a general case while the cylindrical nanotubes are treated as a special class. We found that the chiral indices of a carbon nanotube can always be measured from the electron diffraction pattern regardless if the nanotube is circular or elliptical. An experimental electron diffraction pattern from a partly-deformed carbon nanotube is also analyzed. Assisted with numerical simulations, it is determined that the observed carbon nanotube has chiral indices (15,7) with 8° tilt relative to the horizontal plane and eccentricity of 0.553.

© 2005 Elsevier B.V. All rights reserved.

1. Introduction

Carbon nanotubes have been a focus of intensive studies in materials research for more than a decade since the discovery due to their exceptional mechanical and electrical properties [1,2]. For example, depending on the chiral indices of the nanotube, a carbon nanotube can be either metallic or semiconducting [3–5]. Although carbon nanotubes have the highest tensile strength in the axial direction, they are very flexible and are easily deformed radially [6–9]. Moreover, regardless if a carbon nanotube is metallic or semiconducting, deformation of the nanotube would change its electronic properties drastically such as inducing metal–insulator or insulator–metal transitions [10–12]. For instance, theoretical calculations indicate that the band-gap of a carbon nanotube can be reversibly engineered by radial deformation [11].

As a matter of fact, it is likely in reality that elliptical geometry is more fitting to describe the true structure of nanotubes. Within this framework, nanotubes of circu-

lar cross-section can be considered as a special class of the general elliptical nanotubes of major axis a and minor axis b . When $a = b$, it is the case for circular nanotubes of radius $r_0 = a = b$.

Electron diffraction has been one of the most powerful techniques in determining accurately the atomic structure of both single-walled and multiwalled carbon nanotubes [13–19]. In addition, in the imaging mode, it also offers the capability of locating and identifying morphological features including deformation of carbon nanotubes in detail.

In this Letter, we present a study of the diffraction from elliptical nanotubes with both analytic and numerical analyses. A deformed carbon nanotube that has an elliptical portion is used as an example to illustrate the application of the theoretical method.

2. Theoretical considerations

A carbon nanotube can be considered as pairs of helices along which carbon atoms are distributed in an ordered fashion. In an elliptical carbon nanotube, each helix revolves on the surface of an elliptical cylinder

* Corresponding author. Fax: +1 919 9620480.

E-mail address: lcqin@physics.unc.edu (L.-C. Qin).

which is characterized by its major axis a and minor axis b as shown in Fig. 1. Fig. 1a shows schematically the side-view of a setting of electron diffraction where an elliptical carbon nanotube is tilted with respect to the horizontal plane by an angle β . The analytic expression for the scattering amplitude from an elliptical nanotube is (cf. Appendix A)

$$F(R, \Phi, l) = \sum_j \sum_{n,m} f\eta(n, l) J_n(2\pi R r^*) \exp[in(\Phi^* + \pi/2)] \times \exp[-in\phi_j + 2\pi i l z_j / c], \quad (1)$$

where f is the atomic scattering amplitude for electrons, (ϕ_j, z_j) are the cylindrical coordinates of carbon atoms, J_n is the Bessel function of order n , c is the axial periodicity of the elliptical nanotube, $r^* = \sqrt{a^2 \cos^2 \Phi + b^2 \sin^2 \Phi}$, $\tan \Phi^* = (b/a) \tan \Phi$ and $\eta(n, l) = \int \exp[2\pi i l z(\theta)/c - in\theta] / \sqrt{a^2 \cos^2 \theta + b^2 \sin^2 \theta} d\theta$ is a special function.

In the radial projection, the geometrical relationship between the helices is the same as that for the circular carbon nanotube. For a discontinuous helix on the sur-

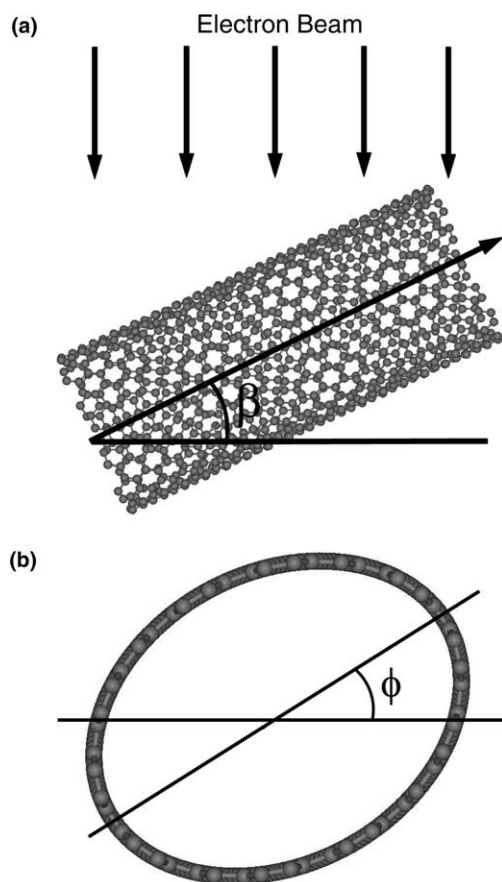


Fig. 1. (a) Schematic showing electron diffraction from an elliptical carbon nanotube in a side view. The tilting angle between the tubule axis and the diffraction plane is β . (b) Cross-sectional view of an elliptical carbon nanotube with ϕ (equal to reciprocal azimuth angle Φ) defining the azimuth angle between the major axis and the diffraction plane.

face of the elliptical nanotube, the pitch length is $C = C_h \tan(60^\circ - \alpha)$ and the axial distance between neighboring atoms on a helix in the axial direction $\Delta = a_0 \sin(60^\circ - \alpha)$, where C_h is the perimeter length and α is the helicity of the nanotube, respectively. Inserting C and Δ into the selection rule Eq. (A.9) in Appendix A, we can obtain the selection rule for an elliptical carbon nanotube (u, v) as

$$l = [n(u + 2v) + 2m(u^2 + v^2 + uv)] / (uM), \quad (2)$$

where M is the maximum common divisor of $(2u + v)$ and $(u + 2v)$. From Eq. (2), we can see that the selection rule is the same for both circular and elliptical nanotubes. This is because the selection rule is only governed by the structural parameters in the axial direction which are not affected by any radial deformation perpendicular to the tubule axis [20]. By taking one atomic helix of the nanotube as a reference $(\phi_0^{(0)}, z_0^{(0)})$, we can have the following rotational and translational shifts for all the helices:

$$\begin{cases} \phi_j^{(0)} = A[(2\pi j a_0 \cos \alpha (1 - e^2)^{1/4} / C_h) | e], \\ z_j^{(0)} = -j a_0 \sin \alpha, \end{cases} \quad (3a)$$

$$\begin{cases} \phi_j^{(1)} = A[(2\pi(j a_0 \cos \alpha + a_0 \sin \alpha / \sqrt{3})(1 - e^2)^{1/4} / C_h) | e], \\ z_j^{(1)} = -j a_0 \sin \alpha + a_0 (\cos \alpha) / \sqrt{3}, \end{cases} \quad (3b)$$

where the superscripts 0 and 1 stand for the two helices within the pair, $A[x|e]$ is an elliptic function which is the inverse function of the elliptic integral of the second kind $E[\phi|e]$ [21], and the subscript j ranges from 0 to $u - 1$ specifying all the u pairs of helices constituting the nanotube. The elliptic function $A[x|e]$ in Eq. (3) is not linear in j . However, since all the parameters in Eq. (3) are independent of R and Φ , we can obtain the scattering amplitude for the elliptical carbon nanotube (u, v) on the layer line l as

$$F_{uv}(R, \Phi, l) = \sum_{n,m} f\eta(n, l) \xi_{uv}(n, m, l) \times \exp[in(\Phi^* + \pi/2)] J_n(2\pi R r^*), \quad (4)$$

where

$$\xi_{uv}(n, m, l) = \sum_j \exp(-in\phi_j + 2\pi i l z_j / c), \quad (5)$$

which can be treated as a constant for a particular Bessel function of order n on layer line l .

The difficulty in expressing $\xi_{uv}(n, m, l)$ in a more explicit analytic form results from the variations of the relative rotational shifts between neighboring helices in an elliptical nanotube. Fig. 2 shows the axial section of an elliptical carbon nanotube. The black dots, standing for the intercepts of the constituting helices, are evenly distributed on the perimeter of the elliptical cylinder.

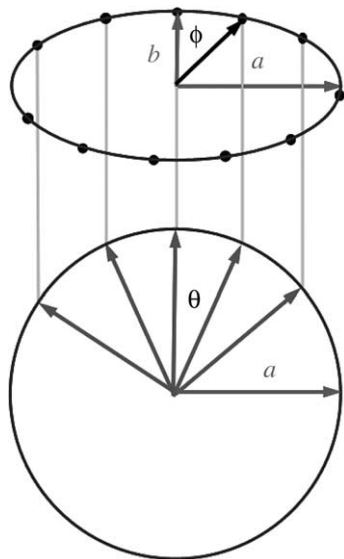


Fig. 2. Schematic illustrating the parameterized expression of an elliptical carbon nanotube in cross-sectional view, with a and b representing the semi-major and semi-minor axis of the ellipse. θ is the parameter defined on a circle and ϕ is the corresponding true angle defined for the ellipse. The black dots on the ellipse are evenly distributed on the perimeter representing the intercepts of the discontinuous atomic helix revolving on the surface of the elliptical nanotube. Although the neighboring dots are equally-distanced, the difference in azimuth angle ϕ between neighboring dots varies with the parameter angle θ .

The relative rotational shifts ϕ_j used in our derivation of the scattering amplitude are expressed by θ in the circle of Fig. 2, where we can see that $\Delta\phi$ between neighboring helices changes significantly. On the other hand, the axial shifts z_j between the constituting helices are exactly the same as those for circular carbon nanotubes, due to the fact that radial deformation does not alter the z -coordinates of carbon atoms in the nanotube.

The electron diffraction patterns of elliptical and circular nanotubes share many similarities. Firstly, the selection rule for elliptical carbon nanotubes (Eq. (2)) is the same as that for circular nanotubes. Secondly, since the diffraction intensity distribution on layer line l is stipulated by $I(R, \Phi, l) = |F(R, \Phi, l)|^2$ and only one Bessel function contributes dominantly to the diffraction layer line l in the experimental data [22], the phase term containing Φ is negligible in the diffraction intensity distribution. This suggests that the chiral indices of an elliptical carbon nanotube (u, v) can still be measured directly from the electron diffraction pattern as for cylindrical carbon nanotubes.

However, it should be noted that the radial variable r^* in Eq. (4) is not a constant. Instead, it is a function of the azimuth angle Φ and therefore the intensity profile of the Bessel function is also dependent on the azimuth angle Φ . The strong dependence on the azimuth angle leads that the symmetry of electron diffraction patterns from an elliptical nanotube may be lower than 2 mm,

especially under inclined incidence, while the electron diffraction patterns of circular nanotubes always has 2mm symmetry [22].

3. Experimental example and discussion

Fig. 3a shows a transmission electron microscope image of a single-walled carbon nanotube. Due to the adsorbed amorphous carbon on the surface, the nanotube is partly deformed as reflected in the narrowing of the measured diameter indicated by the two arrows in the figure. The diameter of this nanotube is measured to be 1.52 nm from the cylindrical section in the image. Fig. 3b is an electron diffraction pattern of the nanotube. There are nine reflection layer lines clearly visible in the diffraction pattern. By measuring the electron scattering intensity distribution and the ratios of the layer line spacings of the principal layer lines, we determined that the nanotube has chiral indices (15,7) of helicity 18.1° and diameter 1.52 nm. It is a semiconducting nanotube.

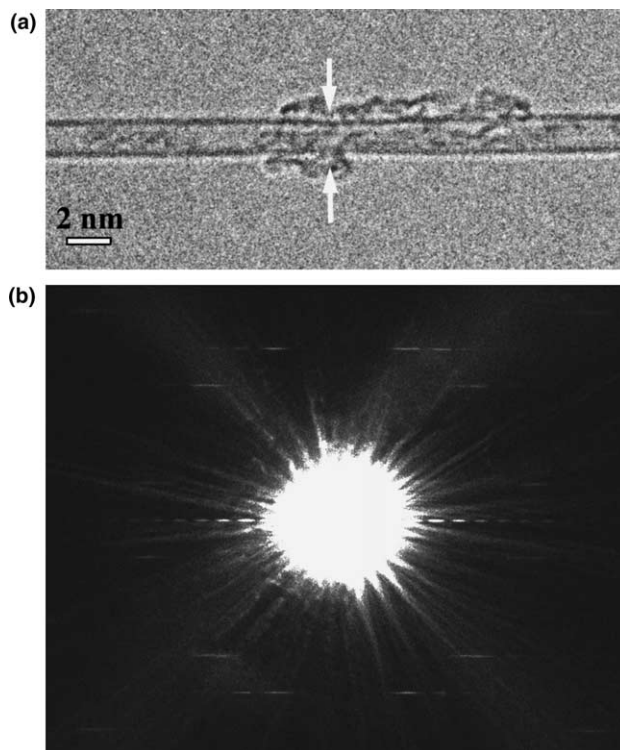


Fig. 3. Transmission electron microscope (TEM) image and electron diffraction pattern of a partly-deformed carbon nanotube (15,7). (a) TEM image of a nanotube of diameter 1.52 nm. The central section of the nanotube is elliptically deformed due to the adsorbed amorphous carbon on the nanotube surface. (b) Electron diffraction pattern of the nanotube. Nine diffraction layer lines are of significant intensities in the diffraction pattern and 2 mm symmetry is absent, indicating that the nanotube is tilted.

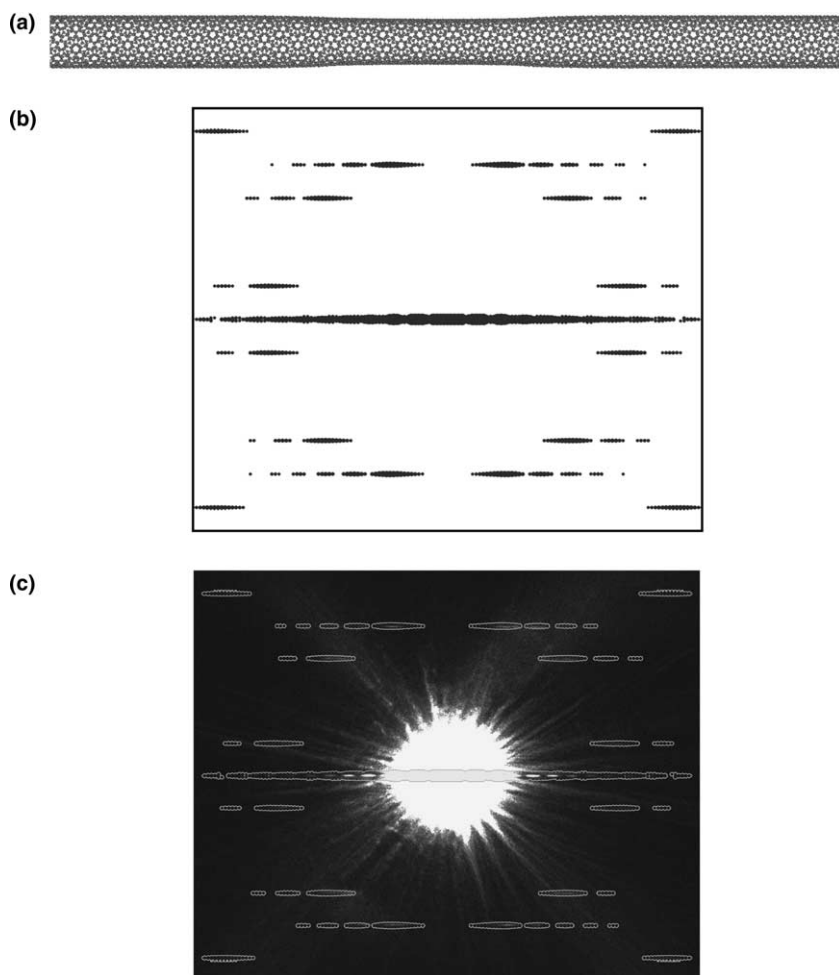


Fig. 4. (a) Model structure of carbon nanotube (15,7) with the central section elliptically deformed by adsorbed carbon molecules. (b) Simulated electron diffraction pattern of the partly-deformed carbon nanotube structure in (a) placed at a tilting angle of 8° with respect to the diffraction plane. (c) Intensity contour of the simulated data shown in (b) plotted on the experimental electron diffraction pattern exhibiting excellent agreement.

Close examination of the diffraction intensity distribution on the principal layer lines in the electron diffraction pattern reveals that the mirror symmetry about the tubule axis is no longer present, due to the elliptical deformation. Fig. 4a shows a model structure of carbon nanotube (15,7) with its central part deformed elliptically. The ratio of a/b for the deformed part is about 1.2 and it corresponds to an eccentricity of $e = \sqrt{1 - b^2/a^2} = 0.553$, which has been considered large enough to change the electrical properties of a carbon nanotube. We have carried out a series of numerical simulations of the electron diffraction intensity distribution at various tilting angles. Fig. 4b shows a simulated electron diffraction pattern from the model structure with a tilting angle $\beta = 8^\circ$. As can be seen in the simulated diffraction pattern, the mirror symmetry across the tubule axis has indeed disappeared due to the tilting of the deformed carbon nanotube relative to the incident electron beam. In Fig. 4c, the profile of the calculated electron diffraction intensities are plotted on the experi-

mental data. The intensity distribution agrees very well for all the layer lines in the diffraction pattern, suggesting that the eccentricity of the nanotube shown in Fig. 3a is about 0.553 with a tilting angle of about 8° relative to the horizontal plane.

It is worth mentioning that the partly-deformed carbon nanotube structure observed experimentally in Fig. 3a is suitable for building carbon-based diode junctions. By controlling the elliptical deformation on the central section of the semiconducting nanotube, this deformed section may become metallic and therefore an insulator–metal–insulator junction could be formed.

4. Conclusions

We have developed a general theory to account for the diffraction from elliptical carbon nanotubes. The chiral indices of a carbon nanotube can be measured directly from the electron diffraction pattern regardless if

the nanotube is circular or elliptical. However, the electron diffraction pattern of an elliptical nanotube may have symmetry lower than 2mm when it is tilted, as illustrated by an experimental electron diffraction pattern from a partly-deformed carbon nanotube of chiral indices (15,7) with eccentricity of 0.553.

Appendix A

The electron scattering amplitude from a coulombic potential $V(r, \phi, z)$ in cylindrical coordinates is [20].

$$F(R, \Phi, Z) = \int V(r, \phi, z) \times \exp[2\pi i(rR \cos(\Phi - \phi) + zZ)] r dr d\phi dz. \quad (\text{A.1})$$

For a continuous elliptical helix, its potential function can be expressed as

$$V(r, \phi, z) = V_0 \delta[r - r_0(\phi)] \delta(z - C\phi/2\pi), \quad (\text{A.2})$$

where V_0 is a constant, C is the pitch length of the helix, and $r_0(\phi)$ is the radial coordinate of the elliptical cylinder that is dependent on the azimuth angle. Using a parameter-based coordinates for the elliptical cylinder defined as

$$\begin{cases} x = a \cos \theta = r \cos \phi \\ x = b \sin \theta = r \sin \phi \\ z(\theta) = \frac{C}{2\pi} \tan^{-1} \left(\frac{b}{a} \tan \theta \right), \end{cases} \quad (\text{A.3})$$

where a and b are the major and minor axes, respectively, of the ellipse of eccentricity $e = \sqrt{1 - b^2/a^2}$. The scattering amplitude for the elliptical helix becomes

$$F(R, \Phi, Z) = \int abV_0 \exp\{2\pi i[Rr^* \cos(\Phi^* - \theta) + Zz(\theta)]\} \frac{d\theta}{\sqrt{a^2 \cos^2 \theta + b^2 \sin^2 \theta}}, \quad (\text{A.4})$$

where $r^* = \sqrt{a^2 \cos^2 \Phi + b^2 \sin^2 \Phi}$ and $\tan \Phi^* = (b/a) \tan \Phi$. Applying the Jacobi–Anger identity

$$\exp[ix \cos \theta] = \sum_{n=-\infty}^{+\infty} J_n(x) \exp[in(\theta + \pi/2)], \quad (\text{A.5})$$

Eq. (A.4) can then be expressed as

$$F(R, \Phi, Z) = \sum_{n=-\infty}^{+\infty} J_n(2\pi Rr^*) \exp \left[in \left(\Phi^* + \frac{\pi}{2} \right) \right] \eta(n, Z), \quad (\text{A.6})$$

where

$$\eta(n, Z) = \int \frac{\exp[2\pi i Z z(\theta) - in\theta]}{\sqrt{a^2 \cos^2 \theta + b^2 \sin^2 \theta}} d\theta. \quad (\text{A.7})$$

Considering the distribution of carbon atoms on the helices and the geometrical relationships (rotational and translational shifts (ϕ_j, z_j)) between all the carbon helices in the elliptical nanotube, the scattering amplitude can finally be expressed as

$$F(R, \Phi, l) = \sum_j \sum_{n,m} f \eta(n, l) J_n(2\pi Rr^*) \times \exp[in(\Phi^* + \pi/2)] \exp[-in\phi_j + 2\pi i l z_j / c], \quad (\text{A.8})$$

where f is the atomic scattering amplitude for electrons and c is the structural periodicity of the elliptical nanotube. This scattering amplitude is subject to the selection rule

$$l/c = n/C + m/\Delta, \quad (\text{A.9})$$

where Δ is the axial distance between neighboring atoms on a continuous helix [20].

For a cylindrical carbon nanotube, $\Phi^* = \Phi$, $\theta = \phi$, and $r^* = r_0$ with r_0 being the radius of the carbon nanotube, and $\eta(n, l)$ becomes a constant.

References

- [1] S. Iijima, Nature (London) 354 (1991) 56.
- [2] M.S. Dresselhaus, G. Dresselhaus, P.C. Eklund, Science of Fullerenes and Carbon Nanotubes, Academic Press, San Diego, 1996.
- [3] N. Hamada, S. Sawada, A. Oshiyama, Phys. Rev. Lett. 68 (1992) 1579.
- [4] J.W. Mintmire, B.I. Dunlap, C.T. White, Phys. Rev. Lett. 68 (1992) 631.
- [5] R. Saito, M. Fujita, G. Dresselhaus, M.S. Dresselhaus, Phys. Rev. B 46 (1992) 1804.
- [6] R.S. Ruoff, J. Tersoff, D.C. Lorents, Nature (London) 364 (1993) 514.
- [7] S. Iijima, C. Brabec, A. Maiti, J. Bernholc, J. Chem. Phys. 104 (1996) 2089.
- [8] V. Lordi, N. Yao, J. Chem. Phys. 109 (1998) 2509.
- [9] J. Tang, L.-C. Qin, T. Sasaki, M. Yudasaka, A. Matsushita, S. Iijima, Phys. Rev. Lett. 85 (2000) 1887.
- [10] A. Rochefort, P. Avouris, F. Lesage, D.R. Salahub, Phys. Rev. B 60 (1999) 13824.
- [11] P.E. Lammert, P. Zhang, V.H. Crespi, Phys. Rev. Lett. 84 (2000) 2453.
- [12] O. Gulseren, T. Yildirim, S. Ciraci, C. Kilic, Phys. Rev. B 65 (2002) 155410.
- [13] L.-C. Qin, T. Ichihashi, S. Iijima, Ultramicroscopy 67 (1997) 181.
- [14] J.M. Cowley, P. Nikolaev, A. Thess, R.E. Smalley, Chem. Phys. Lett. 265 (1997) 379.
- [15] L.-C. Qin, Chem. Phys. Lett. 297 (1998) 23.
- [16] L.-C. Qin, Mater. Characterization 44 (2000) 407.
- [17] J.-F. Colomer, L. Henrard, P. Lambin, G. Van Tendeloo, Euro. Phys. J. B 27 (2002) 111.
- [18] M. Kociak, K. Suenaga, K. Hirahara, Y. Saito, T. Nakahira, S. Iijima, Phys. Rev. Lett. 89 (2002) 155501.
- [19] M. Gao, J.M. Zuo, R.D. Twisten, I. Petrov, L.A. Nagahara, R. Zhang, Appl. Phys. Lett. 82 (2003) 2703.
- [20] L.-C. Qin, J. Mater. Res. 9 (1994) 2450.
- [21] M. Abramowitz, I.A. Stegun, Handbook of Mathematical Functions, National Bureau of Standards, Washington, DC, 1972.
- [22] Z.J. Liu, L.-C. Qin, Chem. Phys. Lett. 400 (2004) 430.